

Bulk motion Comptonization in black-hole accretion flows

Andrzej Niedźwiecki¹ and Andrzej A. Zdziarski²

¹*Lódź University, Department of Physics, Pomorska 149/153, 90-236 Lódź, Poland*

²*Centrum Astronomiczne im. M. Kopernika, Bartycka 18, 00-716 Warszawa, Poland*

Submitted 2005 July 22

ABSTRACT

We study spectra generated as a result of Comptonization of soft photons by cold electrons radially free-falling onto a black hole. We use a Monte Carlo method involving a fully relativistic description of Comptonization in the Kerr space-time. In agreement with previous studies, we find that Comptonization on the bulk motion of free fall gives rise to power-law spectra. In contrast to some previous studies, we find that these power-law spectra extend only to energies much lower than $m_e c^2$. We indicate several effects resulting in generic cutoffs of such spectra at a few tens of keV, regardless of any specific values of physical parameters in the model. Furthermore, the relative normalization of the Compton power law with respect to the peak of black-body disc emission providing the seed photons is in general very low, $\lesssim 10^{-2}$. Then, the inefficiency of producing photons with energies $\gtrsim 100$ keV and the low relative normalization rule out bulk motion Comptonization as a main radiative process in soft spectral states of black-hole binaries.

Key words: accretion, accretion discs – binaries: general – black hole physics – radiation mechanisms: non-thermal – X-rays: stars.

1 INTRODUCTION

Bulk motion Comptonization (BMC) was first considered in a series of papers by Blandford & Payne (1981a, b) and Payne & Blandford (1981). They derived the transfer equation, in the diffusion approximation, for photons repeatedly upscattered by cold electrons undergoing converging inflow. Solution of this equation yields a power-law spectrum with a photon spectral index of $\Gamma = 3$ for the velocity profile corresponding to free fall. Titarchuk & Zannias (1998) and Turolla, Zane & Titarchuk (2002) showed that this property remains valid when effects of general relativity are taken into account. While the above studies demonstrate the ability of this model for producing power-law spectra by scattering on the bulk motion, they do not determine how far such a spectrum extends to high energies. In particular, the Compton recoil and other effects resulting in high energy turnover of the spectrum were not taken into account in those papers.

Notwithstanding the uncertainty about that issue, Chakrabarti & Titarchuk (1995) and Ebisawa, Titarchuk & Chakrabarti (1996) proposed the BMC to be responsible for producing high-energy tails in the soft spectral states of black hole binaries. They argued that both Keplerian and sub-Keplerian (very close to free fall) components are always present in black-hole accretion flows. In the hard state, the latter is hot, and thermal Comptonization dominates. In the soft state, the sub-Keplerian flow remains cold and Comptonization on the bulk motion explains the presence of high-

energy tails, which usually are observed to have $\Gamma \simeq 2.5$ – 3 . Then, application of their BMC model to observational data of several sources was presented by, e.g. Shrader & Titarchuk (1998, 1999) and Borozdin et al. (1999).

On the other hand, e.g., Zdziarski (2000), Zdziarski et al. (2001), McConnell et al. (2002) and Zdziarski & Gierliński (2004) pointed out that the high-energy tails observed in the soft states of black hole binaries extend to energies well above ~ 0.5 MeV (see also Grove et al. 1998; Tomsick et al. 1999; Ueda et al. 2002), without showing any signature of a high-energy cutoff. In particular, the high-energy tail of Cyg X-1 in the soft state shows no cutoff up to at least 10 MeV (McConnell et al. 2002).

There are then some other issues concerning comparison of theoretical implications of the BMC model with data. As pointed out by Zdziarski (2000), Compton reflection (e.g., Magdziarz & Zdziarski 1995) is strong in the soft state of black-hole binaries (e.g., Gierliński et al. 1999), while it should be close to null according to the BMC model. Another problem concerns the relatively large time lags observed and difficult to reconcile with the very small region of the bulk-motion plasma. Furthermore, the presence of the tail in the soft state was claimed to be a unique black hole signature as the BMC process requires the presence of a horizon (e.g., Laurent & Titarchuk 1999, hereafter LT99). However, by now, observations of weakly-magnetized accreting neutron-star binaries in the soft state show high energy

tails to be common in those sources, see, e.g., Farinelli et al. (2005) and references therein.

Still, the cutoff energy seems to be a key feature determining the viability of the model. However, its determination has remained relatively uncertain. The studies dealing with the position of the high energy cutoff include an approximate analytic analysis in Titarchuk, Mastichiadis & Kylafis (1997) and Monte Carlo simulations by LT99 and Laurent & Titarchuk (2001). The Monte Carlo calculations of LT99 have been then compared with the *CGRO/OSSE* soft-state spectra of the black-hole binaries GRO J1655–40 and GRS 1915+105 by Zdziarski (2000) and Zdziarski et al. (2001) respectively, showing that the BMC theoretical spectra fall below of the observed ones at energies $\gtrsim 100$ keV.

We note that Titarchuk et al. (1997) present a simple formula for the cutoff energy derived under the assumption that the cutoff occurs at the energy for which energy gains are balanced by energy losses in the plasma rest frame, but ignoring light bending as well as photon trapping. However, we find that their formula significantly overestimates the cutoff energy even if these effects are not important. Then, LT99 use a fully relativistic description of photon propagation and scattering in the Schwarzschild metric. However, their model appears to oversimplify the treatment of photon transfer in an accreting plasma, as we discuss in Section 2 below.

In this paper, we study formation of BMC spectra using a Monte Carlo method described in Niedźwiecki (2005, hereafter N05) in a model with radially free-falling electrons in a plasma around a black hole. The plasma Comptonizes seed photons from an outer, optically-thick, disc. Our model involves a fully general relativistic (GR) description of photon transfer and Compton scatterings in a plasma located close to a Kerr black hole. In addition, for illustrative purposes, we calculate spectra from a model with photon trajectories approximated by straight lines.

2 THE MODELS

We consider a black hole accreting matter at a mass accretion rate, \dot{M} . The black hole is characterized by its mass, M , and angular momentum, J . We use the Boyer-Lindquist coordinate system $x^i = (t, R, \theta, \phi)$. We also make use of locally non-rotating frames (Bardeen, Press & Teukolsky 1972). The following dimensionless parameters are used in the paper:

$$r = \frac{R}{R_g}, \quad \hat{t} = \frac{ct}{R_g}, \quad \hat{m} = \frac{\dot{M}}{\dot{M}_E}, \quad a = \frac{J}{cR_g M}, \quad (1)$$

where $\dot{M}_E = 4\pi GMm_p/(\sigma_T c)$ is the Eddington accretion rate and $R_g = GM/c^2$ is the gravitational radius. The formalism used by us does not work for $a = 0$ (specifically, the turning point in θ -motion is found according to the formalism described in Chandrasekhar 1983, which requires $a \neq 0$); therefore, spectra for a non-rotating black hole are obtained assuming $a = 10^{-3}$.

We assume that a Keplerian, optically thick disc is replaced by a spherical cloud of free-falling plasma within r_{tr} . In our simulations, we assume a value of $r_{tr} = 20$, for which a relatively high fraction of disc photons is scattered in the

inner cloud. Also, the cloud is assumed to be spherical, neglecting its likely flattening. Both these assumptions maximize the importance of the BMC for spectral formation.

Velocity field of the free-fall, with null angular momentum, is given by

$$u^t = \frac{A}{\Sigma \Delta}, \quad u^r = -\frac{(A - \Delta \Sigma)^{1/2}}{\Sigma}, \quad u^\theta = 0, \quad u^\phi = \frac{2ar}{\Sigma \Delta}, \quad (2)$$

where

$$\Delta = r^2 - 2r + a^2, \quad \Sigma = r^2 + a^2 \cos^2 \theta, \\ A = (r^2 + a^2)^2 - a^2 \Delta \sin^2 \theta, \quad (3)$$

yielding the velocity in the locally non-rotating frame,

$$\beta^r \equiv \frac{v^r}{c} = \frac{A^{1/2}}{\Delta} \frac{u^r}{u^t}, \quad v^\theta = 0, \quad v^\phi = 0, \quad (4)$$

with the corresponding Lorentz factor, $\gamma = [1 - (\beta^r)^2]^{-1/2}$.

We assume that the rest density of electrons, n , is uniform on surfaces of constant r and we determine the density radial profile from the continuity equation. Assuming a pure hydrogen plasma, so that the comoving mass density is $\rho = nm_p$, and integrating the mass conservation equation, we obtain,

$$n(r) = \frac{2\dot{m}}{R_g \sigma_T \int_0^\pi |g|^{1/2} |u^r| d\theta}, \quad (5)$$

where g is the determinant of the metric, $|g| = \Sigma^2 \sin^2 \theta$. Below we use the dimensionless density parameter,

$$\hat{n} \equiv n R_g \sigma_T. \quad (6)$$

For $a = 0$, equations (4) and (5) yield $\beta^r = -(2/r)^{1/2}$ and $\hat{n} = (2/r)^{1/2} \dot{m}/2r$, respectively, and for $a = 0.998$, departures from these profiles are negligible for $r > 3$.

We assume that the electron temperature, T_e , is constant in the inner flow. For most of spectra presented in this paper, we assume $kT_e = 5$ keV, at which the BMC dominates over thermal effects (e.g., Blandford & Payne 1981a; Ebisawa et al. 1996).

In all simulations, seed photons come from thermal emission of the outer, Keplerian, disc. We take into account emission from the area of the disc between r_{tr} and $r_{out} = 100$. The latter value is chosen because illumination of the inner cloud by emission from $r > 100$ is negligible and thus an increase of r_{out} above 100 does not affect resulting BMC spectra. The thermal emission of the disc is modelled as in N05; namely, the point of emission of each photon is generated according to the radial distribution of the disc emissivity and the photon energy is generated from the distribution corresponding to the local temperature. Photons illuminating the region of the free-fall are traced through their consecutive scatterings until they are captured by the black hole or leave the free-fall flow. In modelling Comptonization spectra, we consider two cases, one with photon trajectories approximated by straight lines, and the other with a full GR description of photon motion, hereafter referred to as the flat and GR models, respectively.

Our GR model fully follows the procedure described in N05, involving solution of equations of photon motion in a curved space-time. The optical depth along a photon trajectory in a radially inflowing plasma is given by,

$$d\tau = \hat{n} \frac{\sigma(E_{\text{rest}})}{\sigma_{\text{T}}} \gamma \left(\frac{\Delta\Sigma}{A} \right)^{1/2} \left(\frac{d\hat{t}}{d\zeta} - \frac{A^{1/2}\beta^r}{\Delta} \frac{dr}{d\zeta} \right) d\zeta. \quad (7)$$

This is derived, similarly as in N05, from the elementary expression for the optical depth, $d\tau = n\sigma dl'$, where dl' is the length of photon trajectory measured in the plasma rest frame. In the above equation, ζ is an affine parameter, σ is the Klein-Nishina cross-section averaged over the Maxwellian distribution of electron velocities, E_{rest} is photon energy in the plasma rest frame, and the derivatives $dr/d\zeta$ and $d\hat{t}/d\zeta$ are calculated along the photon trajectory.

On the other hand, photon trajectories in the flat model are approximated by straight lines and the optical depth has the form obtained from equation (7) for $r \gg 1$,

$$d\tau = n\sigma\gamma(1 - \beta^r \cos\phi_r) dl, \quad (8)$$

where ϕ_r is the angle between the outward radial direction and the direction of photon motion and dl is the distance measured by a static observer. All the remaining assumptions in this model are the same as in the GR model, in particular, capture of photons crossing the event horizon (assumed in the flat model at $r_{\text{hor}} = 2$ for $a = 0$). Obviously, our flat model is not self-consistent. We consider it in order to illustrate the crucial impact of space-time curvature on emerging spectra. Also, a number of previous studies neglected the curvature of the space-time and our flat model allows to directly compare these previous results with our Monte Carlo simulations.

Monte Carlo simulations of BMC for both a flat and a GR (with $a = 0$) model were presented in LT99. In both cases, the assumptions underlying their simulations are the same as in this paper. However, we note that their model apparently uses an oversimplified method of integrating the optical depth along photon trajectories valid only for photon transfer in a static plasma in flat space-time. Namely, they use $d\tau = n\sigma dl$, with n being the rest density but dl determined in the Schwarzschild coordinates. Thus, their GR model neglects both the gravitational and kinematic effects affecting the optical depth.

In order to illustrate the significance of the relativistic terms in equation (7), we consider now the optical depth for a *radial* trajectory in the Schwarzschild metric. For $a = 0$ and null angular momentum of a photon, equation (7) yields

$$d\tau = \sigma n \gamma (1 \pm \beta^r) (1 - 2/r)^{-1/2} dr. \quad (9)$$

The last two terms give the proper length in the Schwarzschild geometry, $g_{rr}^{1/2} dr$, where $g_{rr} = (1 - 2/r)^{-1}$, and $\gamma(1 \pm \beta^r)$ gives the Lorentz transformation from the plasma rest frame. For the free-fall velocity field, $\beta^r = -(2/r)^{1/2}$, and then equation (9) yields

$$d\tau = \frac{\sigma n dr}{1 \pm (2/r)^{1/2}}. \quad (10)$$

The upper and lower sign in equations (9) and (10) corresponds to ingoing ($dr/d\zeta < 0$) and outgoing photons, respectively. (Note that the optical depth remains finite for ingoing photons at the event horizon.)

On the other hand, the optical depth for a radial trajectory in LT99 is given as $\sigma n dr$, see, e.g., eq. (2) in that paper. Such simplified treatment yields roughly two times higher optical depth than our equation (10) for ingoing photons, while for photons escaping from the vicinity of the event

horizon, it underestimates τ by a factor of a few. Equation (10) implies a significant decrease of the probability of escape from the innermost region of a free-falling flow with respect to the non-relativistic approach. The latter may result in strongly overestimated emission from the inner region. In Section 3.4 below, we indicate this effect as a possible explanation for discrepancies between results of our model and LT99 at high accretion rates.

3 RESULTS

Spectra emerging in models with $r_{\text{tr}} = 20$, $kT_e = 5$ keV, $M = 10M_{\odot}$ and various accretion rates are shown in Fig. 1(a–d) for the flat model and in Fig. 1(e–h) for the GR model with a non-rotating black hole. In all the models, the luminosity of the Comptonization component is smaller than 4 per cent of the total luminosity. (This fraction drops below 1 per cent when the transition occurs at the marginally stable orbit, $r_{\text{tr}} = 6$.) We also show contributions from photons scattered in various parts of the inner flow.

3.1 The cutoff energy in the flat model

In the flat model, the cutoff energy decreases with increasing \dot{m} , starting from ~ 100 keV at low accretion rates to a few tens of keV at $\dot{m} \gtrsim 10$. As illustrated on Fig. 1(a–d), this decrease of the cutoff energy is primarily related to the diminishing contribution of radiation emerging from inner parts of the flow. In the flat model, the innermost parts generate radiation extending to highest energies. However, the optical depth for photons moving outward in the innermost region is typically a few times higher than for photons moving inward, as discussed in Section 2. As a result, photons at high accretion rates are trapped in the inner flow and carried under the event horizon. Such a trapping effect has been considered, e.g., by Begelman (1979) and Payne & Blandford (1981), who defined the trapping radius, $r_{\text{trap}} \sim \dot{m}$, as the distance at which the diffusion velocity equals the flow velocity.

An increase of \dot{m} results then in an increase of the trapping radius and depletion of increasing number of photons from the high-energy part of the spectrum. Moreover, photons which diffusively escape from the region inside r_{trap} lose significant fraction of their energy in scatterings, compare the dashed and the heavy solid curves in Fig. 1(d). In the flat model, the position of the trapping radius is crucial for the dependence of the cutoff energy on the accretion rate.

We note that the formula derived in Titarchuk et al. (1997) for BMC in flat space-time, $E_{\text{cut}} = [4/\dot{m} + (4/3)(v^r/c)^2]m_e c^2$ [note that the form of the second term in eq. (9) of Titarchuk et al. (1997) is valid only for a plasma with $v^r = -(2/r)^{1/2}c$; we use a more general form which can be derived from Appendix D of their paper], predicts the cutoff energies a few times higher than these found in our simulations even when setting $v^r = 0$. The cause for that discrepancy is that their analysis ignores photon trapping and is based on the assumption that the cutoff occurs at photon energies for which energy gains are balanced by Compton recoil. We find that although the average increase of photon energy in a scattering indeed increases with decreasing \dot{m}

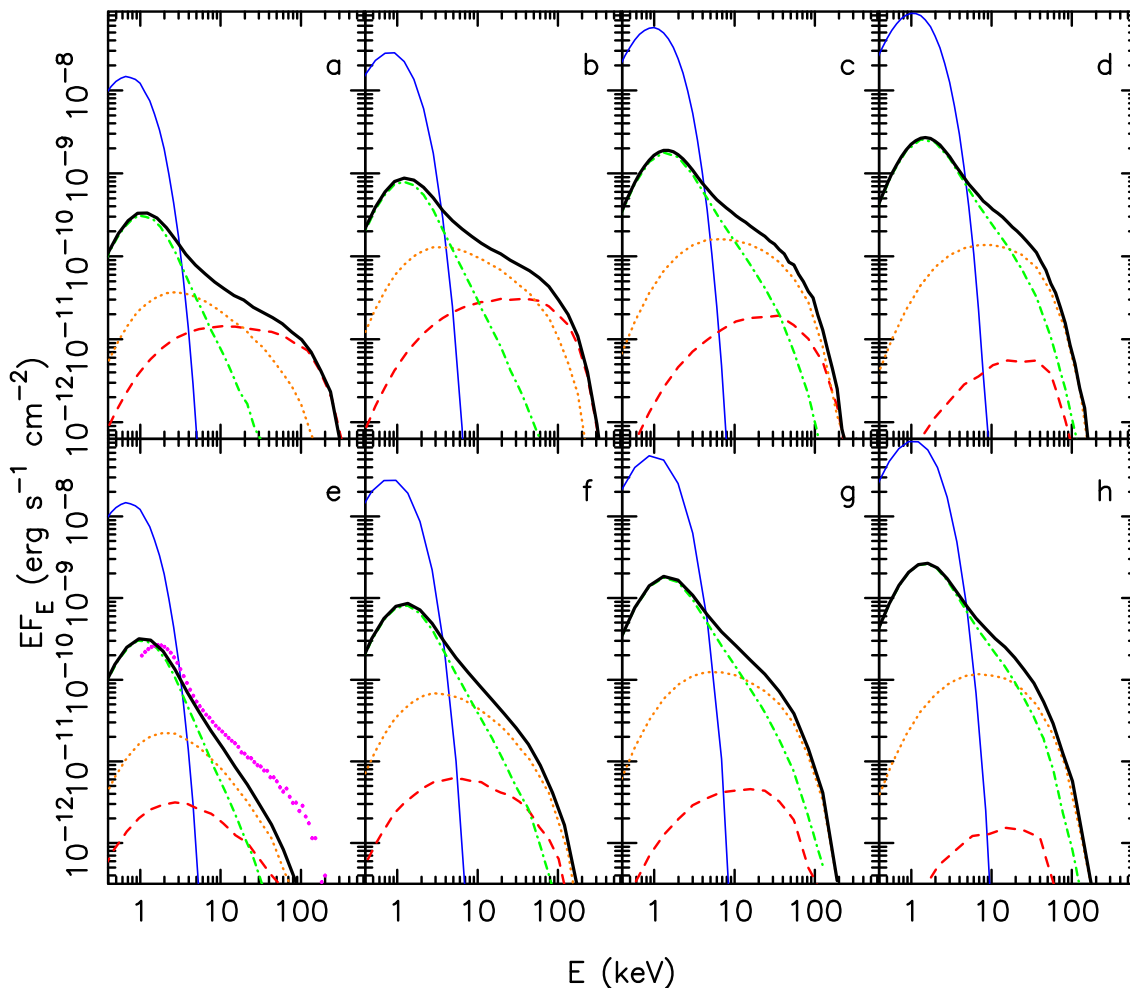


Figure 1. Emerging spectra for models with a Keplerian disc outside $r_{\text{tr}} = 20$ and a spherical, free-falling, cold ($kT_e = 5$ keV) inflow inside r_{tr} . The unscattered part of the blackbody disc emission and Comptonization spectra are shown by the thin (blue online) and heavy (black) solid curves, respectively. All spectra are angle-averaged and correspond to a black hole with $M = 10M_\odot$ at a distance of $d = 5$ kpc. The accretion rate is $\dot{m} = 2, 4, 8$ and 12 from left to right. The top panels show spectra for the flat model, and the bottom panels are for the GR model with a non-rotating black hole. The dashed (red), dotted (orange) and dot-dashed (green) curves show contribution from photons for which the smallest scattering radius is within $r = 2-5, 5-8,$ and $8-20,$ respectively. The (magenta) points in (e) show the spectrum for $\dot{m} = 2$ and $kT_e = 5$ keV obtained by LT99 in their GR model.

(as lower density results in higher velocity gradient between scatterings), the above formula strongly overestimates the cutoff energy. Even at low accretion rates, $\dot{m} < 4$, for which trapping is not important, the formula is not consistent with our results, yielding unrealistic values of the cutoff energy, $E_{\text{cut}} > 500$ keV, regardless of the value of the radial velocity.

3.2 The cutoff energy including space-time curvature

The spectra in the GR model are cut off below 100 keV for all values of the \dot{m} , see Fig. 1(e-h). Thus, bending of photon trajectories strongly diminishes the contribution from the innermost region with respect to the flat model. This is due to several effects.

As explained below, basic properties of photon motion imply that for $a = 0$ all photons emerging from the flow from $r \leq 5$ (i.e., those avoiding crossing the horizon) are strongly redshifted when reaching a distant observer. Therefore, the

emission from the $r = 2-5$ region contributes negligibly to the overall spectrum in the GR model with $\dot{m} = 2$, in spite of the trapping surface being very close to the event horizon, whereas this region gives a major contribution to the 20–200 keV spectrum in the corresponding flat model, as illustrated in Figs. 1(a) and (e).

The energy observed by a distant observer, E_{inf} , is related to the photon energy in the plasma rest frame, E_{rest} , by

$$E_{\text{inf}} = (1 - 2/r)^{1/2} \gamma (1 - \beta^r \cos \Phi_r) E_{\text{rest}}, \quad (11)$$

where Φ_r is the angle between the inward radial direction and the photon direction in the plasma rest frame. Taking into account that the Lorentz factor for $\beta^r = -(2/r)^{1/2}$ reduces with the gravitational redshift, $(1 - 2/r)^{1/2}$ (i.e., their product is unity), we obtain,

$$E_{\text{inf}} = [1 + (2/r)^{1/2} \cos \Phi_r] E_{\text{rest}}, \quad (12)$$

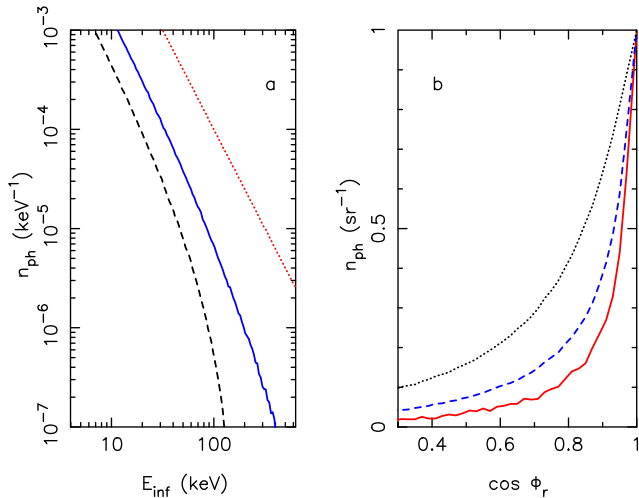


Figure 2. (a) The dashed (black online) and solid (blue online) curves show the angle-averaged spectrum of photons escaping to infinity that experience scattering taking place at $3.5R_g$ in the Schwarzschild and extreme Kerr geometry, respectively, off target electrons with the free-fall velocity ($v^r \approx -0.75c$ for both geometries). The incident photons, with the power-law spectrum shown by the dotted (red) line, move in the inward radial direction. (b) The angular distribution of photons in the local rest frame scattered within the inner $5R_g$ for $\dot{m} = 4$. The number of photons per unit solid angle is given as a function of the angle of the photon direction before scattering with respect to the radial direction ($\cos \Phi_r = 1$ corresponds to the inward direction). The dashed (blue) and solid (red) curves show photons with the initial energy corresponding to $E_{\text{inf}} < 40$ keV and > 40 keV, respectively, in the GR model. The dotted (black) curve is for photons with $E_{\text{inf}} > 40$ keV in the flat model. All the curves are normalized to unity at $\cos \Phi_r = 1$.

which implies that only photons emitted inward in the plasma rest frame ($\Phi_r < \pi/2$) are observed as blueshifted.

On the other hand, the half-angle of the cone of avoidance, as defined in Chandrasekhar (1983),

$$\tan \Phi = (r/2 - 1)^{1/2} (r/3 - 1)^{-1} (r/6 + 1)^{-1/2} \quad (13)$$

corresponds to $\Phi_r = \pi/2$ [for which the aberration of light gives $\tan \Phi = 1/(\gamma|\beta^r|)$] at $r = 5.2$. Then, all photons escaping from $r < 5.2$ must be emitted backward and thus they have $E_{\text{inf}}/E_{\text{rest}} < 1$. The above constraint is valid for $a = 0$. For $a = 0.998$ such an effective redshift of all escaping photons is restricted only to emission from $r < 2$.

Another reason for the inefficiency of BMC is that the velocity corresponding to the free-fall is relatively small in the region where most of high energy emission is generated. In the GR model, the major contribution to the high energy part of the spectrum comes from photons scattered within $r = 5-8$, where velocity is at most mildly relativistic, $v^r \approx 0.5-0.7c$.

Finally, we point out the importance of an additional effect, occurring for photons undergoing scattering in the Klein-Nishina regime, which severely reduces emission of hard X-rays. Namely, the highest energies are achieved by photons scattered toward the center, which then must be scattered off the inward direction to escape the flow. However, photons are preferentially scattered forward (and subsequently captured) at high energies. Then, photons which

significantly change direction in a scattering, so that they can escape, lose much of their energy to the recoil. Furthermore, the decline of the Klein-Nishina cross section makes scattering of high-energy photons less probable.

Fig. 2(a) shows the spectrum at infinity due to scattering of radially incoming photons with an initial power-law spectrum at $r = 3.5$. Below 40 keV, the flux of escaping radiation is over an order of magnitude lower than the illuminating flux due to capture of the scattered photons. Above 40 keV, the preference of forward scattering combined with the Compton recoil result in a sharp cutoff in the spectrum.

Fig. 2(b) shows the angular distribution of photons undergoing scattering within inner $5R_g$, found in our Monte Carlo simulation for models with $\dot{m} = 4$. The incident photons are strongly concentrated along the inward radial direction, and this concentration increases with the increasing photon energy. Such an anisotropic radiation field makes the above effects, depleting hard X-ray photons from radiation outgoing from the innermost region, crucial for the spectrum. Note the related steepening, above ~ 40 keV, of spectra shown by dashed curves in Figs. 1(e-f). On the other hand, the concentration of photons in the radial direction is less pronounced in the flat model and thus the above effect is less important.

3.3 Black hole spin

Both the radial velocity and density profiles changes with varying a are negligible for the considered spherical free-falling plasma. A significant impact of the space-time metric on BMC spectra arises only due to properties of photon trajectories in the vicinity of the event horizon. The number of photons escaping from the innermost region increases with the increasing a for other parameters unchanged. Furthermore, the escaping photons have slightly higher blueshifts at higher values of a . For example, in the case of $a = 0.998$, the maximum blueshift, $E_{\text{inf}}/E_{\text{rest}} = 1.5$, is obtained for photons escaping from $3 < r < 8$, while for $a = 0$, the maximum blueshift increases from 1 at $r = 5.2$ to 1.3 at $r = 8$. Such differences in photon motion make the steepening of the high-energy part of the spectrum generated by scattering at $r = 3.5$ in the extreme Kerr metric less pronounced than in case of the Schwarzschild metric, see Fig. 2(a).

Fig. 3 compares spectra at infinity in models with $a = 0$ and $a = 0.998$ for the same accretion rates. In general, Comptonization spectra show very weak dependence on a . The strongest dependence may be expected for low \dot{m} , for which photons generated close to the event horizon are not trapped. For $\dot{m} = 0.5$, Fig. 3(a), the spectra in models with $a = 0.998$ and $a = 0$ are dominated above 15 keV by emission from $r < 5$ and $5 < r < 8$, respectively. However, the related difference between these spectra is rather moderate; most noticeably, the cutoffs occur at ~ 30 and ~ 50 keV for $a = 0$ and 0.998, respectively. Note also that for such low values of \dot{m} , the BMC process is very inefficient, yielding spectra with $\Gamma \gtrsim 4$. For $\dot{m} \geq 4$, the spectra are dominated by photons for which the last scattering takes place at relatively large values of r , where the differences between low and high a are small. This makes the black hole spin weakly important for the spectrum.

Strong gravity effects may affect dynamics of Compton scattering in the ergosphere of a rapidly rotating black hole

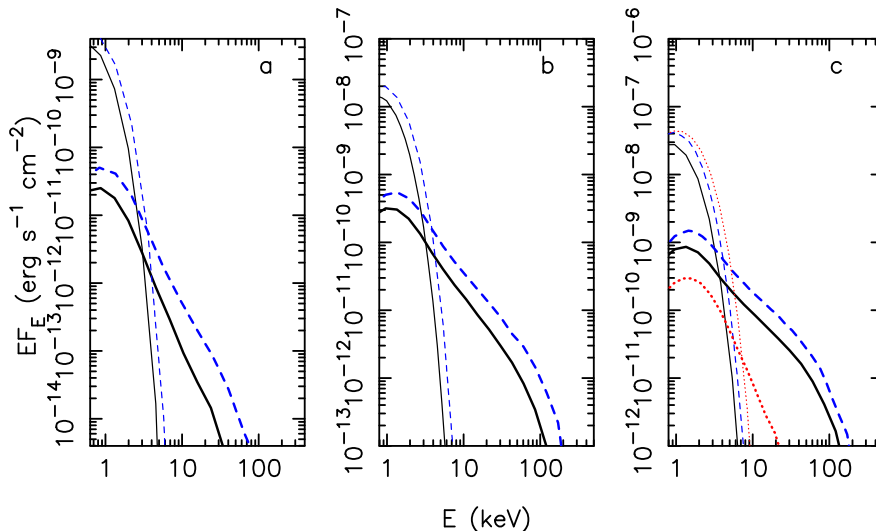


Figure 3. The solid (black online) and dashed (blue online) curves show spectra for the GR model for $a = 0$ and $a = 0.998$, respectively. The $\dot{m} = 0.5$ (a), 2 (b), 4 (c), and $r_{\text{tr}} = 20$, $M = 10M_{\odot}$, $kT_e = 5$ keV. The thin and heavy curves show the emission from the thermal disc and from the BMC, respectively. The dotted (red online) curves in (c) are for the GR model with $r_{\text{tr}} = 6$, $\dot{m} = 4$ and $a = 0$.

(Piran & Shaham 1977). We find, however, that such effects are not important for the formation of BMC spectra due to strongly relativistic radial velocities. Ergospheric emission of a cold free-falling plasma is strongly collimated inward and it does not give any significant contribution to the observed spectrum. Thus, we confirm a conclusion of N05 that a quasi-Keplerian motion is needed to make radiative processes in the ergosphere important for spectral formation.

3.4 Spectral index

For all spectra, we determine the photon spectral index, Γ , in the 10–30 keV energy range. Below 10 keV, contribution from thermal Comptonization with $kT_e = 5$ keV is important, and significant departures from a power-law occur in some models above 30 keV.

The values obtained by us for $\dot{m} > 4$ in the GR model and for $\dot{m} > 8$ in the flat model agree with the $\Gamma = 3$ of the solution of the transfer equation in the diffusion approximation (e.g., Payne & Blandford 1981). At low accretion rates, spectra of the flat model are harder, $\Gamma \simeq 2.6$ for $\dot{m} \leq 4$, due to the strong contribution from the innermost region. On the other hand, spectra emerging at low accretion rates in the GR model are much softer, $\Gamma \gtrsim 3.5$ for $\dot{m} \leq 2$.

A steepening with decreasing \dot{m} also characterizes spectra obtained by LT99 for their GR model with $kT_e = 5$ keV (see table 2 in LT99). However, their spectra are harder than ours at any accretion rate. At high accretion rates, $\dot{m} > 4$, the difference is moderate, $\Gamma = 2.8$ in LT99 vs. $\Gamma = 3$ in our model, and we find that it could be accounted for by our improved treatment of photon transfer (see Section 2). Indeed, we achieved spectra with $\Gamma = 2.8$ for $\dot{m} > 4$ with equation (7) replaced by $d\tau = n\sigma dl$. The same conclusion is valid for the flat model. Table 1 in LT99 gives $\Gamma = 2$ for their flat model with $\dot{m} = 7$ and $kT_e = 5$ keV, while our calculations yield $\Gamma = 2.7$ at this \dot{m} . However, neglecting the relativistic terms in equation (8), we obtain similarly hard

spectra, with $\Gamma = 2.2$ at $\dot{m} \geq 4$, approximately accounting for the difference.

At low accretion rates, discrepancies between our models and those of LT99 become more significant, and we have found no explanation for them. In particular, we obtain $\Gamma = 3.6$ for $\dot{m} = 2$ whereas LT99 find $\Gamma = 2.9$. Both of those spectra are compared on Fig. 1(e). The (unphysical) modification of $d\tau$ described above does not resolve this discrepancy. We stress, however, that those discrepancies remain unimportant for our overall conclusions.

Furthermore, LT99 conclude that the change of the size of the region containing free-falling plasma between $r_{\text{tr}} = 6$ and 40 has weak effects on the spectra. We find an opposite property: the spectra soften significantly when r_{tr} drops below 10. For r_{tr} approaching the marginally stable orbit ($6R_g$ for $a = 0$), the spectra soften by at least $\Delta\Gamma = 1$ with respect to those shown in Fig. 1, as illustrated by the lower dotted curve in Fig. 3(c). The reason for that is obvious; as shown in Fig. 1, a major part of the high energy emission is generated in the flow beyond $6R_g$. Then the Comptonized component becomes much weaker and softer if the flow shrinks to $r_{\text{tr}} = 6$.

On the other hand, we confirm the conclusion of LT99 that the illumination pattern does not affect significantly the emerging spectra. By replacing emission from the whole surface of the outer disc by emission from the inner edge (at r_{tr}), we obtain similar slopes, although the latter approach does not allow us to determine the normalization of the Comptonized emission with respect to the disc thermal component.

3.5 BMC vs. thermal Comptonization

Fig. 4 compares a BMC spectrum with spectra for semi-relativistic thermal Comptonization. For $kT_e \gtrsim 10$ keV, thermal Comptonization completely dominates formation of spectra and the role of bulk motion is negligible (see also Jaroszyński 2001).

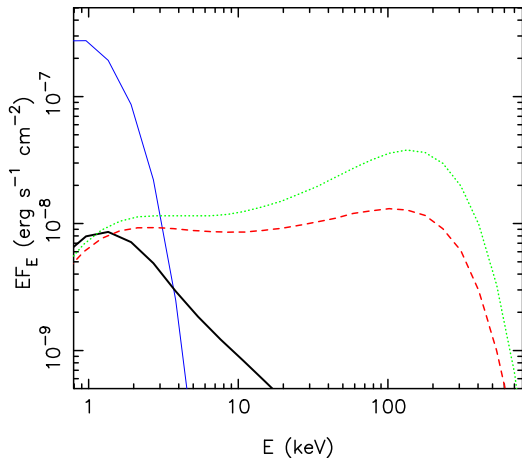


Figure 4. The dotted (green online) and dashed (red) curves show Comptonization spectra from static and free-falling, respectively, plasmas at $kT_e = 50$ keV. The heavy solid (black) curve shows the spectrum from a free-falling plasma with $kT_e = 5$ keV. The free-fall spectra are for $\dot{m} = 4$ and the static plasma spectrum is for the same density distribution. The $a = 0$, $r_{\text{tr}} = 20$ and $M = 10M_\odot$ in all models. The thin (blue) solid curve shows the blackbody disc emission, which is the same for all three models.

Fig. 4 also compares spectra from thermal Comptonization between static and free-falling plasmas with the same rest density distributions. The major impact of rapid accretion on formation of thermal Comptonization spectra is due to trapping of photons in optically thick regions of inflowing plasma, making a Wien bump much less pronounced, which effect has been studied by Colpi (1988).

4 DISCUSSION AND CONCLUSIONS

We have examined formation of spectra emerging due to multiple scattering of photons in black-hole accretion flows with relativistic radial velocities. In agreement with previous studies, we find that this model gives rise to power-law spectra with the photon spectral index $\Gamma \approx 3$ at high accretion rates.

We point out effects preventing this power-law from extending beyond 100 keV. The recoil effect, dominant at lower accretion rates in flat space-time, results in a cutoff around 100 keV. At higher accretion rates, trapping of photons reduces contribution of photons from innermost regions. In a curved space-time, bending of photon trajectories combined with an increased probability of forward scattering at high energies result in cutoffs at a few tens of keV even at low accretion rates. We find that rotation of the black hole has a minor effect on the BMC spectra.

We do not confirm claims of, e.g., Titarchuk et al. (1997) and LT99 that the power-law spectrum extends to $\sim m_e c^2$. We find that such high energies are achieved only by photons scattered at very small r toward the center which do not contribute to observed spectra.

We also stress that the normalization of the BMC spectral component with respect to the peak of the disc blackbody spectrum is very low, typically $\lesssim 10^{-2}$. If a likely flattening of the free-falling plasma were taken into account, this relative normalization would become even lower. Thus, the

process is unable to explain the high energy tails of black-hole binaries in the soft state, which have usually much higher amplitudes (see, e.g., Zdziarski & Gierliński 2004), even regardless of the position of the high-energy cutoff. This property of the BMC process has not been obvious from previous studies, as, e.g., the spectral figures in LT99 do not show the disc blackbody component. We also caution that the implementation of BMC in the X-ray data fitting code XSPEC allows for an arbitrary normalization of the Comptonization tail (as well as it does not include any high-energy cutoff), in contrast to the theoretical results.

On the other hand, a BMC spectral component can be observable in ultrasoft (i.e., strongly dominated by a disc blackbody) states of black-hole binaries (e.g., Gierliński & Done 2004). In those spectral states, a high-energy tail beyond the disc blackbody is either currently unobservable or very weak. However, a high-energy tail due to the BMC process may become observable with increasing sensitivity of future X-ray detectors. In fact, a tail with the relative amplitude low enough for the BMC process has already been observed in some cases, see e.g., fig. 8 in Zdziarski & Gierliński (2004), although it appears to be too hard in some cases, e.g., having $\Gamma \sim 2$ in GRS 1915+105 (Zdziarski et al. 2001).

ACKNOWLEDGEMENTS

We thank Ph. Laurent for supplying his Monte Carlo results. This paper was supported through KBN grants 1P03D01827, 1P03D01727, 4T12E04727 and PBZ-KBN-054/P03/2001.

REFERENCES

- Bardeen J. M., Press W. H., Teukolsky S. A., 1972, ApJ, 178, 347
- Begelman M. C., 1979, MNRAS, 187, 237
- Blandford R. D., Payne D. G., 1981a, MNRAS, 194, 1033
- Blandford R. D., Payne D. G., 1981b, MNRAS, 194, 1041
- Borozdin, K., et al. 1999, ApJ, 517, 367
- Chakrabarti S. N., Titarchuk L., 1995, ApJ, 455, 623
- Chandrasekhar, S., 1983, The Mathematical Theory of Black Holes. Oxford Univ. Press, Oxford
- Colpi M., 1988, ApJ, 326, 223
- Ebisawa K., Titarchuk L., Chakrabarti S., 1996, PASJ, 48, 59
- Farinelli R., Frontera F., Zdziarski A. A., Stella L., Zhang S. N., van der Klis M., Masetti N., Amati L., 2005, A&A, 434, 25
- Gierliński M., Done C., 2004, MNRAS, 347, 885
- Gierliński M., Zdziarski A. A., Poutanen J., Coppi P. S., Ebisawa K., Johnson N. W., 1999, MNRAS, 309, 496
- Grove J. E., Johnson W. N., Kroeger R. A., McNaron-Brown K., Skibo J. G., Philips B. F., 1998, ApJ, 500, 899
- Jaroszyński M., 2001, Acta Astronomica, 51, 91
- Laurent P., Titarchuk L., 1999, ApJ, 511, 289 (LT99)
- Laurent P., Titarchuk L., 2001, ApJ, 562, L67
- Magdziarz P., Zdziarski A. A., 1995, MNRAS, 273, 837
- McConnell M. L., et al., 2002, ApJ, 572, 984
- Niedźwiecki A., 2005, MNRAS, 356, 913 (N05)
- Payne D. G., Blandford R. D., 1981, MNRAS, 196, 781
- Piran T., Shaham J., 1977, Physical Review D, 16, 1615
- Shrader C., Titarchuk L., 1998, ApJ, 499, L31
- Shrader C., Titarchuk L., 1999, ApJ, 521, L121
- Titarchuk L., Mastichiadis A., Kylafis N. D., 1997, ApJ, 487, 834
- Titarchuk L., Zannias T., 1998, ApJ, 493, 863

- Tomsick J. A., Kaaret P., Kroeger R. A., Remillard R. A., 1999, ApJ, 512, 892
- Turolla R., Zane S., Titarchuk L., 2002, ApJ, 576, 349
- Ueda Y., et al., 2002, ApJ, 571, 918
- Zdziarski A. A., 2000, in P. C. H. Martens, S. Tsuruta & M. A. Weber, eds., IAU Symp. 195, Highly Energetic Physical Processes and Mechanisms for Emission from Astrophysical Plasmas. ASP, San Francisco, p. 153 (astro-ph/0001078)
- Zdziarski A. A., Gierliński M., 2004, Progr. Theor. Phys. Suppl., 155, 99
- Zdziarski A. A., Grove J. E., Poutanen J., Rao A. R., Vadawale S. V., 2001, ApJ, 554, L45